Fin Bending due to Stress and its Simulation

Alp H. Gencer, Dimitrios Tsamados and Victor Moroz
Synopsys, Inc. Mountain View, CA
alpg@synopsys.com

***Abstract*— Modern CMOS and memory devices feature fins, which are high aspect ratio elements. While narrow and tall fins enhance electrical characteristics, they are mechanically weak structures. Unexpected failure mechanisms, such as fin bending and even cracking can arise in such devices. This paper discusses such mechanisms and offers a methodology to simulate them.**

Keywords— Fin bending, leaning, FinFET, stress engineering

I. INTRODUCTION

In the recent years, FinFETs have become quite popular for state of the art CMOS technologies, with several foundries and IDMs moving to FinFET technology for their most advanced technology node [1]. Moreover, modern memory devices feature deep trenches with tall and narrow active areas in shape of fins [2]. Such devices offer significant electrical performance and smaller area advantages for technology nodes below 28/32nm.

Even though fin-based structures may be superior electrically, they are less robust than planar structures mechanically, which may give rise to some unexpected failure mechanisms [3,4]. One such mechanism, fin bending, is discussed in this paper.

II. EFFECTS OF MECHANICAL STRESS ON FIN SHAPE

In a fin-based structure, stress can arise due to difference in thermal expansion coefficients of various materials used or due to intrinsic stress of deposited layers. Since stress can enhance the mobility of carriers, device designers deliberately introduce intrinsically stressed layers into the process in order to achieve better electrical performance. This technique, which is widely used for planar transistors, can be applied to FinFETs as well.

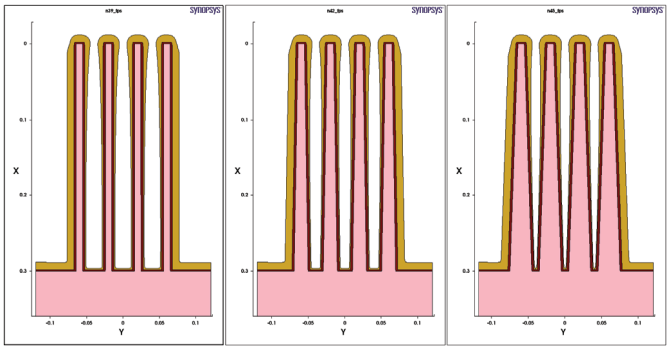

Figure 1: Non-uniform cap layer deposition due to narrow space between the fins.

If a single fin is in isolation with no other structure around it, different stress distributions can arise based on the shape of the fin, but present no problem to the structural integrity of the device, since the effect is symmetric. However, FinFETs are usually manufactured not as a single fin, but in multiple fins in order to achieve the desired device width. The space between the fins is kept to a minimum, and the fins are made as high as possible to get the best current/surface area ratio. This would mean that when a cap layer is deposited, the area between the fins may not be covered uniformly (Fig. 1).

As a consequence of this asymmetry in the thickness of the cap layer, combined with the intrinsic stress or thermal stress, the thin fins can actually bend. The outermost sides of the fins get a thicker cap layer, such that the fins tend to bend outwards.

III. ANALYTICAL MODEL FOR VERIFICATION

In order to verify the validity of the simulations for fin bending due to asymmetrical deposition, an analytical model is derived for the calculation of the displacement along the transversal direction of a rectangular beam. The derivation of the model has been based on [5]. The structure used for the model is a rectangular fin with two deposited layers of differing thickness, one on each side as presented in Fig. 2.

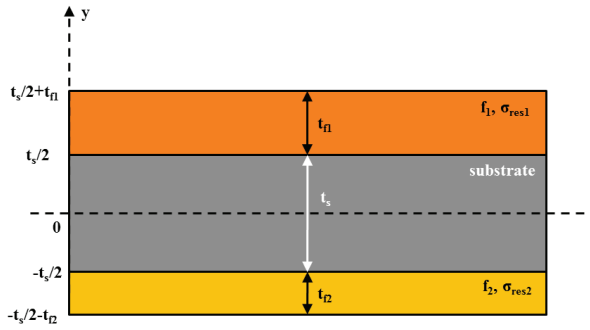

Figure 2: Schematic cross-section of a fin covered on both sides by asymmetrically deposited layers.

The basic assumptions are that there are no residual stresses in the substrate (fin) but only in the two layers covering it on both sides (f_1 and f_2). Those stresses can be intrinsic or thermally induced due to the difference of the coefficients of thermal expansion between the layers and the fin. For biaxial stresses the Young's modulus has to be replaced by the biaxial modulus E/(1-v) where v is the Poisson ratio. Following the same reasoning as in [5] we derive the quantities of the uniform strain component c, the location of the bending axis t_b, (that is the line along which the bending strain is zero) and the curvature radius r of the fin from the mechanical equilibrium equations:

$$E_s\, t_s\, c + E_{f1}\, t_{f1}\, c + \sigma_{res1}\, t_{f1} + E_{f2}\, t_{f2}\, c + \sigma_{res2}\, t_{f2} = 0$$

$$\Rightarrow c = -\frac{\sigma_{res1}\, t_{f1} + \sigma_{res2}\, t_{f2}}{E_s\, t_s + E_{f1}\, t_{f1} + E_{f2}\, t_{f2}} \quad (1)$$

$$\int_{-\frac{t_s}{2}-t_{f2}}^{-\frac{t_s}{2}} \frac{E_{f2}\,(y - t_b)}{r}\, dy + \int_{-\frac{t_s}{2}}^{\frac{t_s}{2}} \frac{E_s\,(y - t_b)}{r}\, dy + \int_{\frac{t_s}{2}}^{\frac{t_s}{2}+t_{f1}} \frac{E_{f1}\,(y - t_b)}{r}\, dy = 0$$

$$\Rightarrow t_b = \frac{E_{f1}\, t_{f1}\left(t_{f1} + t_s\right) - E_{f2}\, t_{f2}\left(t_{f2} + t_s\right)}{2\left(E_s\, t_s + E_{f1}\, t_{f1} + E_{f2}\, t_{f2}\right)} \quad (2)$$

$$\int_{-\frac{t_s}{2}-t_{f2}}^{-\frac{t_s}{2}} \sigma_{f2}\,(y - t_b)\, dy + \int_{-\frac{t_s}{2}}^{\frac{t_s}{2}} \sigma_s\,(y - t_b)\, dy + \int_{\frac{t_s}{2}}^{\frac{t_s}{2}+t_{f1}} \sigma_{f1}\,(y - t_b)\, dy = M \quad (3)$$

where:

$\sigma_{f2} = \sigma_{res2} + E_{f2}\left(c + \frac{(z - t_b)}{r}\right)$, $\sigma_s = E_s\left(c + \frac{(z - t_b)}{r}\right)$ and $\sigma_{f1} = \sigma_{res1} + E_{f1}\left(c + \frac{(z - t_b)}{r}\right)$

From (3) we get after some quite lengthy calculations:

$$\frac{A}{r} + B = M \Rightarrow \frac{1}{r} = \frac{M - B}{A} \quad (4)$$

where:

$$A = E_{f1}\, t_{f1}\left[\frac{t_s^2}{4} + \frac{t_s\, t_{f1}}{2} + \frac{t_{f1}^2}{3} - t_s\, t_b - t_{f1}\, t_b + t_b^2\right] + E_s\, t_s\left[\frac{t_s^2}{12} + t_b^2\right] + E_{f2}\, t_{f2}\left[\frac{t_s^2}{4} + \frac{t_s\, t_{f2}}{2} + \frac{t_{f2}^2}{3} + t_s\, t_b + t_{f2}\, t_b + t_b^2\right]$$

and $B = \left(\sigma_{res1} + E_{f1}\, c\right) t_{f1}\left(\frac{t_s + t_{f1}}{2} - t_b\right) - E_s\, t_s\, t_b\, c - \left(\sigma_{res2} + E_{f2}\, c\right) t_{f2}\left(\frac{t_s + t_{f2}}{2} + t_b\right)$

In the case when the displacement at the tip of the fin (d) is much smaller than its height (L) then the radius of curvature of the fin (r) is connected to the displacement at the tip of the fin with the following equation:

$$d \cong \frac{L^2}{2\, r} \Rightarrow d \cong \frac{L^2}{2}\frac{M - B}{A} \quad (5)$$

From the equation above we observe that the displacement is linearly dependent on the residual stresses in the layers. If no external force (moment) is applied to the structure M=0 and the displacement equation is further simplified to:

$$d \cong -\frac{L^2}{2}\frac{B}{A}$$

The comparison with simulation results shows an excellent agreement for both uniaxial and biaxial stresses. In Fig. 3 the displacement d is shown as a function of the biaxial stress for a fin with a width of 50nm and asymmetric oxide of 20nm and 15nm width on either side. The displacement in the 3D Sentaurus Interconnect simulation (Fig. 4) is extracted in the middle of the fin's tip. In both uniaxial and biaxial stresses the discrepancy between the simulation and the analytical model is less than 1%. The structure used for the comparison of the analytical and numerical models has been meshed with second order elements in order to reduce the number of mesh elements and maintain an excellent level of accuracy (Fig. 5).

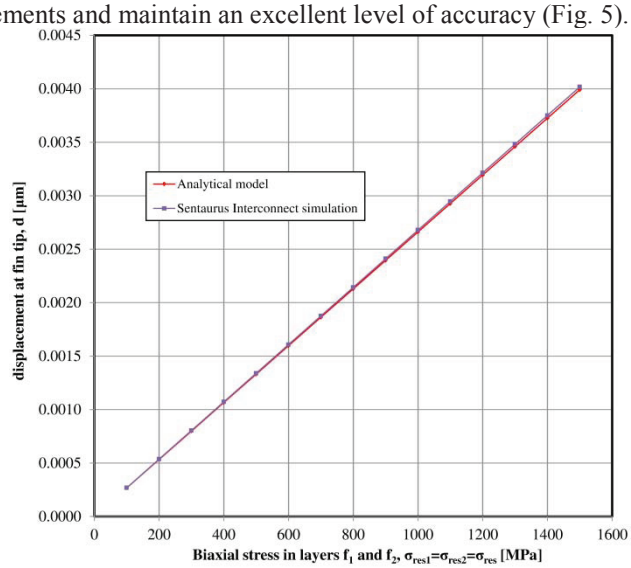

Figure 3: Graph presenting the displacement of the fin's tip as a function of the biaxial intrinsic stress of the deposited layers.

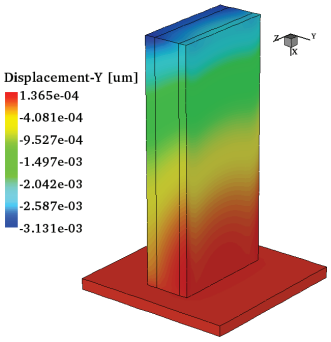

Figure 4: The displacement in the y direction mapped on the 3D structure of the simplified fin.

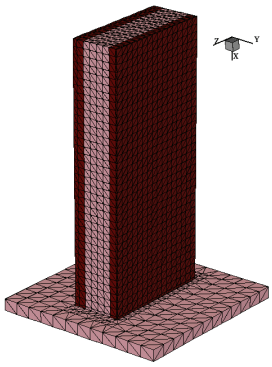

Figure 5: Meshing used for the simplified fin simulation in Sentaurus Interconnect showing second order elements

IV. Simultaneous Simulation of Asymmetric Deposition and Fin Bending

We use Sentaurus Topography to simulate the asymmetric deposition process using LPCVD. The stress distribution and resulting structural deformation is simulated with Sentaurus Interconnect. Since both deposition and bending occur simultaneously, we use a loop to deposit a portion of the cap layer, simulate bending, deposit some more and then simulate bending again. Through switching between the two tools in a loop, the desired bending effect can be simulated.

The progress of bending over several iterations can be observed in Fig. 6. The bending process makes the space between the fins larger, allowing for a more uniform cap layer deposition, such that the bending process is slowed and eventually stops.

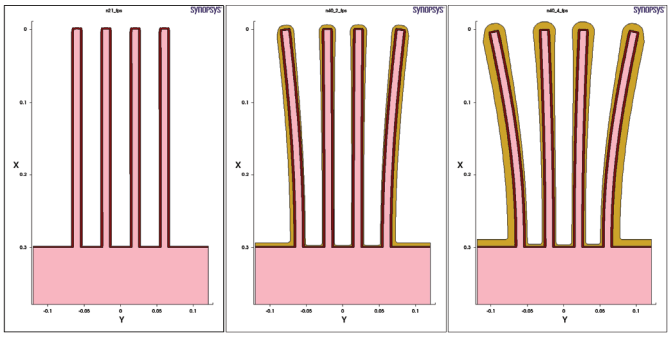

Figure 6: Progressive bending of fins due to non-uniformly distributed cap layer stress.

V. Deposition and Bending Simulations in 3D

After the obtaining 2D results, the next step was to create a more realistic fin structure using Sentaurus Topography 3D in conjunction with Sentaurus Interconnect mechanics solver. First the fin is patterned using an RIE-like etch algorithm in Sentaurus Topography that created the structure as in Fig. 7.

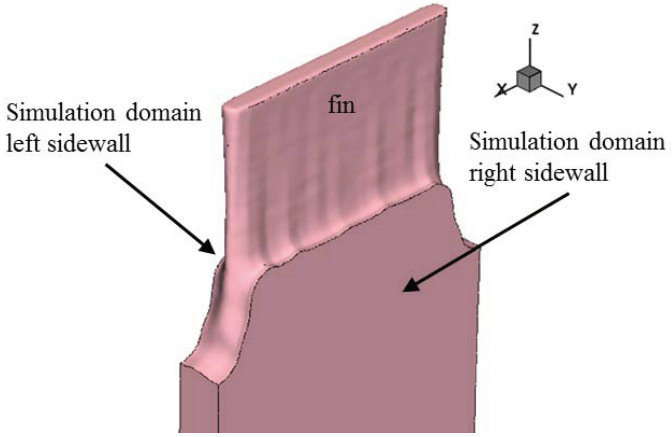

Figure 7: Etched fin using an RIE algorithm in Sentaurus Topography 3D.

The finalized fin model is then imported in Sentaurus Interconnect where an oxide layer has been deposited in 5 steps. Sentaurus Topography 3D has been used in the background for this deposition with an algorithm emulating an LPCVD. In order to save simulation time, reflective boundary conditions (BCs) are used at the sidewalls for the calculation of the flows of particles in Sentaurus Topography 3D. The distance of the fin's walls from the simulation domain boundaries (sidewalls, Fig. 8) dictate its distance from its (virtual) neighboring fins on each side. By introducing a slight offset of the fin from one of the simulation sidewalls the flow of particles is modulated on each side of the fin and an asymmetrical deposition of oxide is produced. Consequently, if an intrinsic stress is applied in the deposited oxide then a mechanical moment is created in the fin and the fin is bent towards one of its sides: Towards the thinner for compressive stresses and the thicker for tensile – see Fig. 9 with compressive stress of 900MPa.

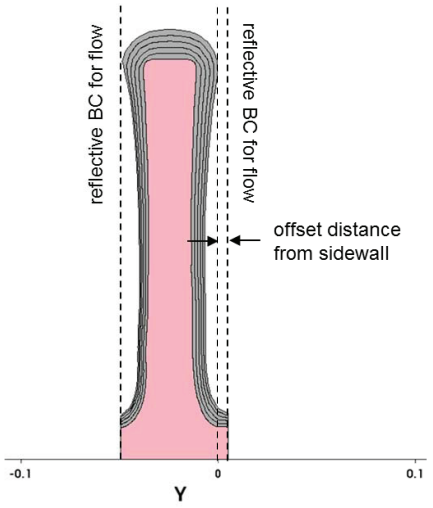

Figure 8: Fin's cross-section showing the offset distance introduced from the right sidewall in order to create an asymmetrical deposition of material.

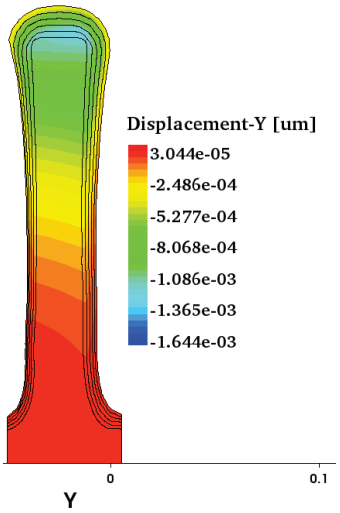

Figure 9: The asymmetrically deposited material with an intrinsic stress of -900MPa creates a mechanical moment in the fin and a displacement of its tip toward the thinner-layer side.

Table 1

Intrinsic stress in layers [MPa]	Displacement in y-direction [nm] (simulation)	Displacement y-direction [nm] (model)	Diff. (%)	Dimensions of the fin & layer mean thicknesses
-300.0	0.390	0.365	6.8	L=185nm
-450.0	0.592	0.547	8.2	t_s=25nm,
-600.0	0.789	0.729	8.2	w=320nm
-750.0	0.985	0.912	8.0	t_{f1}=6.57nm,
-900.0	1.183	1.094	8.1	t_{f2}=4.30nm

In Table 1, a comparison of the extracted displacement of the fin's tip in the middle with respect to the analytical model is presented for various compressive stress values. We observe that due to the small height of the fin and the small thickness of the layers the displacements are rather small. Even though the fin is not rectangular as before, the agreement with the

analytical model is quite satisfactory with a discrepancy of the order of 8%.

We have to bear in mind that the displacements at the fin edges tend to be slightly bigger than in the middle as the biaxial stresses bend the fin along its longitudinal axis (along the x-axis as seen in Fig. 10). That means that the longer the fin (increasing w) the more bowing and displacement at the fin's tip edges are to be expected. In Fig. 11 the normal stress distribution in the x direction is shown on a single 3D fin. Simulations of more than one fins are possible as shown in Fig. 12 but are computationally more expensive and are avoided if the periodicity and the symmetry of the fin arrays permit it.

VI. Effects of Inconsistent Fin Spacing

Fins are usually manufactured using self-aligned double patterning (SADP) using a spacer. SADP ensures that the fin width is uniform along the length of the fin. However, if there are inconsistencies in the width of the lines that are used for SADP, e.g. due to line edge roughness, the spacing between the fins can be inconsistent, even though the fins themselves have uniform width. This is another source of inconsistency in the cap layer thickness and is another reason for bending.

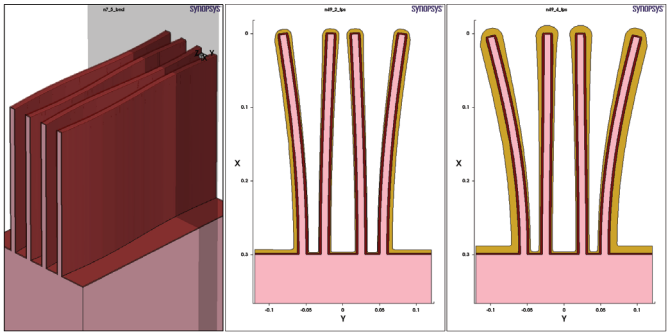

Figure 13: Fin bending behavior of irregularly spaced fins due to line edge roughness in SADP.

Such a structure is shown in Fig 13. Due to line edge roughness, in cross-section C1 the spacing between the middle fins is larger than the nominal value, whereas the spacing between the outer fins is smaller than the nominal value. In this case, the inner fins tend to bend inwards, since the large inner spacing causes a thicker layer deposition. However, as the fins bend, the inner spacing gets smaller and the outer fin spacing gets larger, reversing the process to some degree.

VII. Conclusions

In modern FinFETs and memory devices with fins, it is important to ensure structural integrity of the fins. Even small variations in fin spacing can cause unexpected bending and device failure. Careful design of the fin shape and of the fin spacing, assisted by simulation, can help designers to avoid such issues. The simulation not only can predict bending, but also the final stress distribution, which is important for mobility enhancement calculations.

References

[1] Kuhn, K.J., "CMOS scaling for the 22nm node and beyond: Device physics and technology," *International Symposium on VLSI Technology, Systems and Applications (VLSI-TSA),* pp.1, 2011.

[2] Kim, J.-Y., et. al, "S-RCAT (sphere-shaped-recess-channel-array transistor) technology for 70nm DRAM feature size and beyond," Symposium on VLSI Technology, pp.34 2005.

[3] Prall, Kirk, "Scaling Non-Volatile Memory Below 30nm". In Proceedings of Non-Volatile Semiconductor Memory Workshop, 2007.

[4] Prall, Kirk and Parat, Krishna, "25nm 64Gb MLC NAND Technology and Scaling Challenges". In Proceedings of IEDM, 2010..

[5] Hsueh C.-H., "Modeling of elastic deformation of multilayers due to residual stresses and external bending", Journal of Applied Physics, vol.91, no. 12, pp.9652-9656, 2002

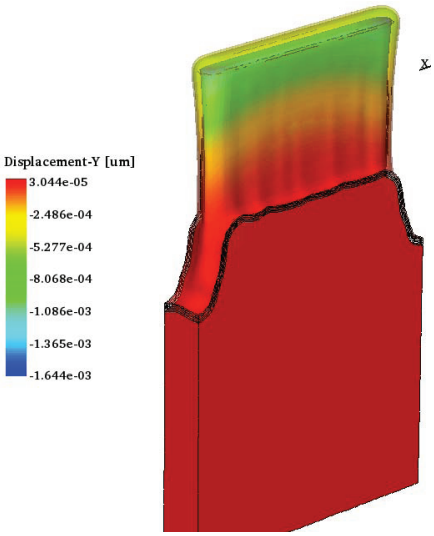

Figure 10: 3D structure with the displacements in the y-direction mapped upon.

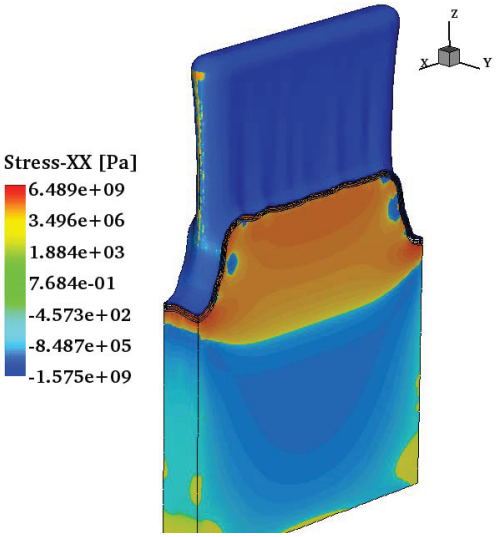

Figure 11: Normal component of stress along the x-direction.

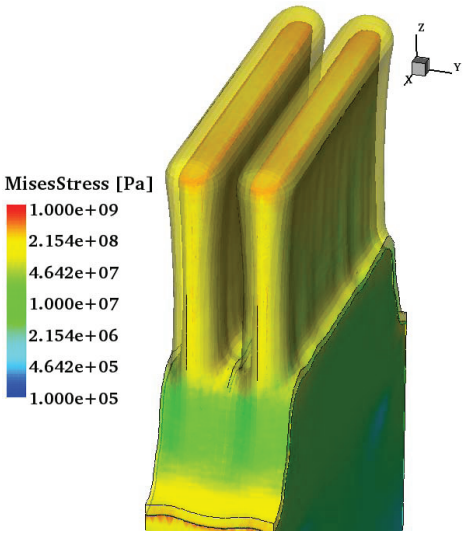

Figure 12: Pressure distribution in a pair of fins and in the deposited layers.